Fine Chemical Engineering
http://ojs.wiserpub.com/index.php/FCE/

Research Article

# Synthesis of Novel Bacterial Cellulose Based Silver-Metal Organic Frameworks (BC@Ag-MOF) as Antibacterial Wound Healing

**Nathania Puspitasari[1,2*], David Arief[3], Suryadi Ismadji[1,2], Vienna Saraswaty[2,4], Shella Permatasari Santoso[1,2], Ery Susiany Retnoningtyas[1], Jindrayani Nyoo Putro[1,2], Chintya Gunarto[1,2]**

[1]Department of Chemical Engineering, Widya Mandala Surabaya Catholic University, Surabaya, Indonesia
[2]Collaborative Research Center for Zero Waste and Sustainability, Widya Mandala Surabaya Catholic University, Surabaya, Indonesia
[3]Department of Chemical Engineering, National Taiwan University of Science and Technology, Taipei, Taiwan
[4]Research Centre for Applied Microbiology, National Research and Innovation Agency Republic of Indonesia, Cibinong, Indonesia
E-mail: nathania.puspita@ukwms.ac.id

**Received:** 27 May 2023; **Revised:** 11 July 2023; **Accepted:** 18 July 2023

**Abstract:** Bacterial Cellulose (BC) is a polymer derived from the bacterium *Komagataeibacter xylinus* with great potential for biomedical applications due to its high biocompatibility and biodegradability. In addition, the polymer is naturally biosynthesized by bacteria as hydrogels which can be used as optimal substrates for wound healing. However, the drawback of BC is the absence of antibacterial properties. Nowadays, some infections become more prevalent and harder to treat because of antimicrobial resistance, therefore, it is necessary to develop a strategy for modifying BC as wound healing that provides protection against bacterial contamination. In this work, silver-based Metal Organic Frameworks (MOFs) were immobilized into Bacterial Cellulose (BC). MOFs are porous coordination materials consisting of metal ions and multidentate organic ligands that have the potential as a matrix for metal ions due to their ability to gradually release metal ions. The structure and morphology of BC@Ag-MOF were successfully confirmed by Fourier-Transform Infrared spectroscopy (FTIR) and Scanning Electron Microscope (SEM). Evidently, BC@Ag-MOF exhibited a higher silver content (63.19%) than BC@Ag without immobilization into MOF (48.46%). Therefore, it indicated that MOF has large pores for enhancing the capacity for silver ion absorption in BC. The modified BC has never been reported and achieved the highest antibacterial activity of 99.99% against Gram-negative bacteria *Escherichia coli*. Moreover, BC@Ag-MOF has a higher antibacterial efficiency of 97% compared to BC@Ag without matrix. This study expands the potential application of BC modification in the field of biological antibacterial.

***Keywords*:** bacterial cellulose, zeolitic imidazolate framework-8, silver, antibacterial, *Escherichia coli*

## 1. Introduction

The development and application of natural polymer-based wound healing have been investigated in recent years. Bacterial Cellulose (BC) from *Komagataeibacter xylinus* become one of the excellent wound healing agents.[1-3] The material is biocompatible, which is non-toxic, does not cause allergies, and can accelerate wound healing.[4,5] Bacterial cellulose gel has been utilized in skin transplantation and other wound treatments as a part of the healing process. The


DOI: https://doi.org/10.37256/fce.4220233120

usefulness of BC as a medical product was investigated in various publications.[6,7] To fulfill standards as a wound healing agent, it is necessary to modify BC by increasing its antibacterial activity. Microorganisms, especially *Escherichia coli* have potential to become a significant public health problem for various diseases such as Urinary Tract Infection (UTI), cholecystitis, and other clinical infections.[8] In the majority of biological applications, lowering the risk of infection is crucial. BC has a high-water holding capacity and porosity, allowing it to absorb and release antimicrobial solutions gradually. Thus, the synthesis of BC-based antibacterial wound healing can be achieved by antibiotic impregnations, nanoparticles, or polymers that have antimicrobial activity.[9-11]

Metal nanoparticles have attracted great interest and are typically applied in various industrial sectors because of their unique optical, catalytic, and biological features.[12-14] Currently, microbially synthesized nanoparticles have been recognized as a cost-effective and environmentally friendly method and are suitable for large-scale production. Various kinds of microbes such as fungi, algae, and bacteria can release proteins, enzymes, and organic molecules that work as stabilizing and reducing agents for metal ions.[15,16] Among various metal nanoparticles, silver nanoparticles (AgNPs) have attracted much attention for applications in various fields, including biosensing materials, biomedicine, and wound dressings.[17-19] In addition, AgNPs are known as strong antibacterial agents due to their cytotoxic effects against various bacteria, the inhibition rate reached 100% at 125 ppm of AgNPs.[20] However, AgNPs aggregation in solution and duration of recovery are considered two critical challenges for the broad application of these nanoparticles. Therefore, many strategies have been used to overcome this problem, including the encapsulation and immobilization of AgNPs in various matrices.[21-23] On the other hand, MOFs have been widely applied for the detection of food or water contaminants, photo-fenton degradation of organic pollutants, the improvement of membranes performance, and immobilization of metal nanoparticles.[24-31] MOFs are crystalline compounds consisting of metal ions and organic ligands and have attracted much attention through its properties such as high porosity and large surface area.[32,33] One type of MOF, Zeolitic Imidazolate Framework-8 (ZIF-8), can be used as a promising antibacterial matrix with large pore size and ability to release metal ions.[34-36] So far, composite pellicle of BC@Ag-MOF has not been reported yet. The objective of this research was to investigate novel bacterial cellulose based silver-metal organic frameworks and its potential for antibacterial wound healing against Gram-negative *E. coli*.

## 2. Materials and methods

### 2.1 *Materials and strain*

*Komagataeibacter xylinus* strain ATCC 11142 that produced bacterial cellulose was supplied by Bioresource Collection and Research Center (BCRC) (Hsinchu, Taiwan). The Hestrin and Schramm (HS) medium, which contains 2.7 g/L $Na_2HPO_4$, 5 g/L yeast extract, 1.15 g/L citric acid, 20 g/L glucose, and 5 g/L peptone was used for bacterial cultivation at 30 °C. All analytical grade chemicals used in this research were obtained from Merck, Sigma, and Acros.

### 2.2 *Synthesis of BC@Ag-MOF*

After 1 week of cultivation, the BC membrane was separated from the media and pre-treated with alkaline method to remove the residual biomass. Cellulose pellicle was treated with 1 M NaOH for 2 h at 90 °C three times and rinsed with distilled water until a neutral pH was reached. The BC pellicle obtained was 1.5 × 1.5 $cm^2$ according to the diameter of the test tube used.

ZIF-8 crystals were synthesized by slowly pouring of 10 mmol of $Zn(NO_3)_2 \cdot 6H_2O$ into 40 mmol of 2-methylimidazole and stirred the mixture for 5 minutes. Finally, the mixture was allowed to stand for 24 hours at room temperature, centrifuged at 6,000 rpm, and dried at 50 °C overnight to obtain ZIF-8 crystals. In the Ag-MOF synthesis, the material was prepared by mixing $AgNO_3$ and MOFs solutions (1:1 ratio) with various concentrations of each component 5, 15, and 25 mM. Then, the mixture was stirred using a magnetic stirrer at room temperature (150 rpm) for 2 hours. Subsequently, the BC pellicle was immersed in Ag-MOF solution for 2 hours. The modified material (BC@Ag-MOF) was rinsed with distilled water three times followed by drying process using a freeze dryer prior to characterization.

## 2.3 *Characterizations*

Field Emission Scanning Electron Microscopy (FE-SEM) was used to determine the surface morphology of modified BC samples (JSM-6500F, JEOL, Japan). While Fourier-Transform Infrared spectroscopy (FTIR) (FTS 3500, Bio-Rad Laboratories Sadtler Division, USA) was employed to analyze the chemical composition of samples with the wavenumber of 4,000-400 $cm^{-1}$.

## 2.4 *Antibacterial test*

The antibacterial activity of modified BC was tested against Gram-negative *Escherichia coli* by the following two methods. In disc diffusion method, the samples were sterilized by autoclaving for 15 minutes at 120 °C. A total of 100 $\mu$L *E. Coli* solution with $OD_{600}$ 0.1 was spread onto an agar plate, then the samples were attached to the agar surface and incubated at 37 °C overnight to form inhibition zone.

In Colony Forming Unit (CFU) method, *E. coli* cultures were inoculated in Luria Broth (LB) media at 37 °C overnight. The Bacterial cells were separated from the media by centrifugation and washed twice with NaCl solution pH 6.5. The bacterial solution was diluted to a final concentration of $OD_{600}$ 1 with NaCl solution. Samples were mixed with a total of 10 mL bacterial solution for 30, 60, and 120 minutes at 37 °C. Subsequently, 100 $\mu$L of bacterial supernatant with appropriate dilution was added to the LB agar plate. The samples were incubated at 37 °C and bacterial colonies were counted after 24 hours of incubation.

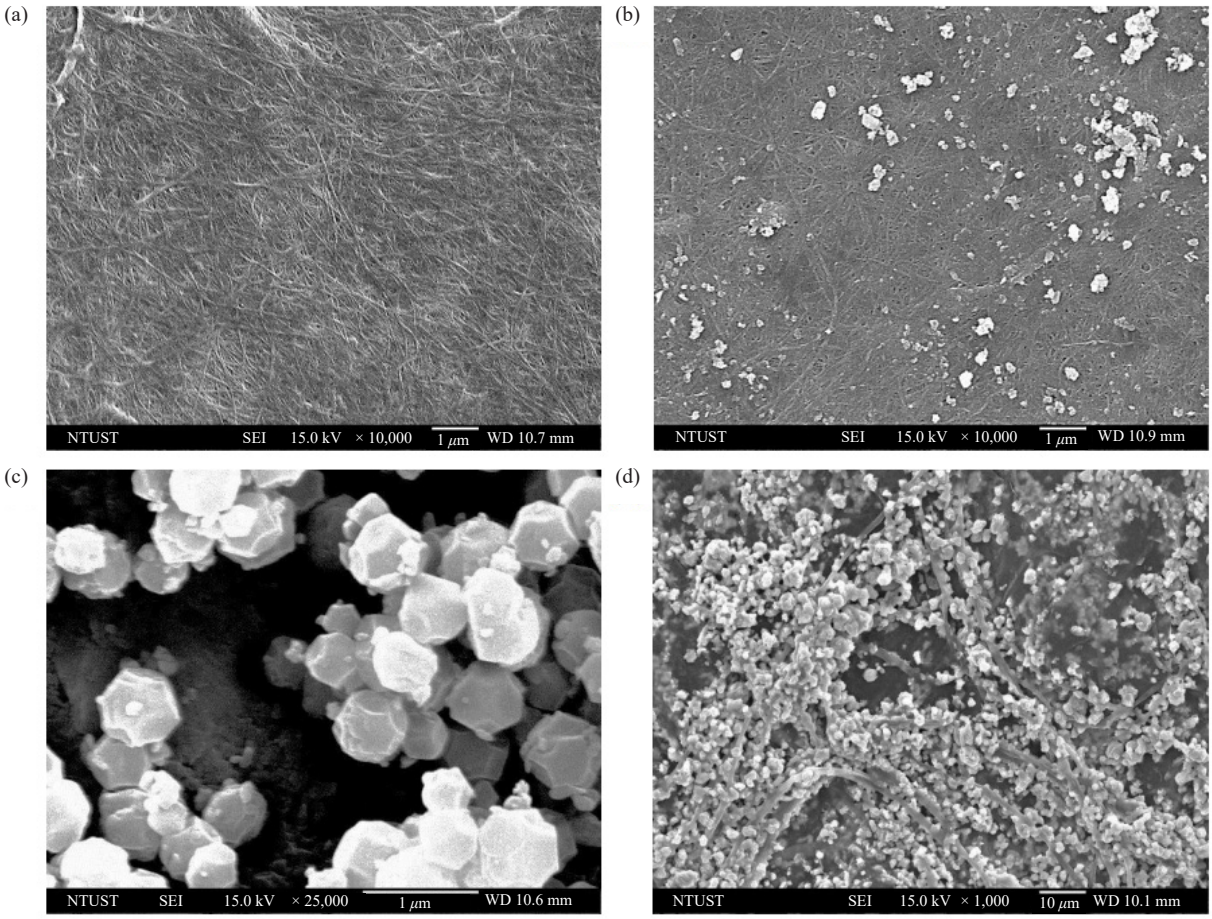


**Figure 1.** SEM analysis of (a) BC (10,000×), (b) BC@Ag with concentration of $AgNO_3$ 25 mM (10,000×), (c) ZIF-8 (25,000×), (d) BC@Ag-MOF with concentrations of $AgNO_3$ and ZIF-8 (1:1) 25 mM (1,000×)

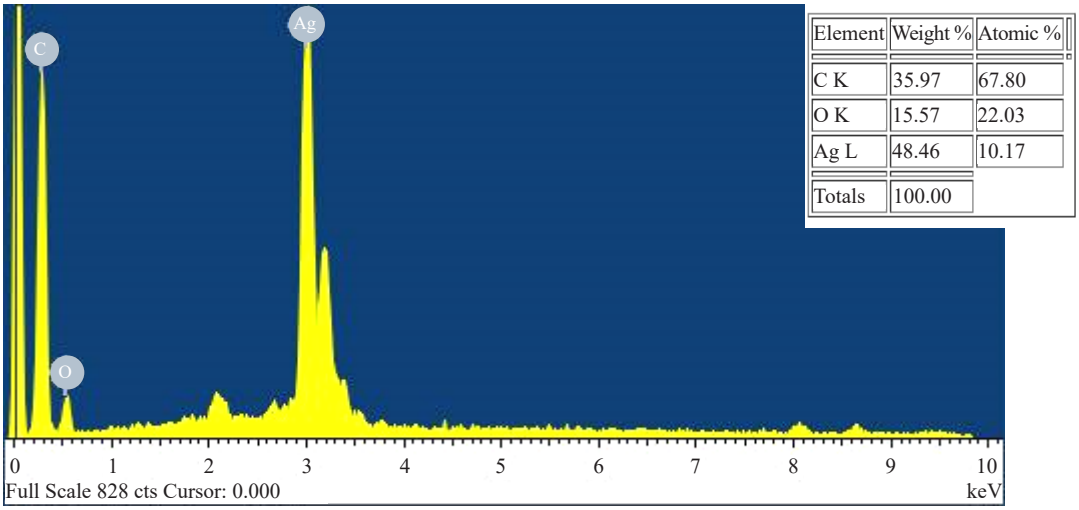


| Element | Weight % | Atomic % |
|---|---|---|
| C K | 35.97 | 67.80 |
| O K | 15.57 | 22.03 |
| Ag L | 48.46 | 10.17 |
| Totals | 100.00 | |

(a)

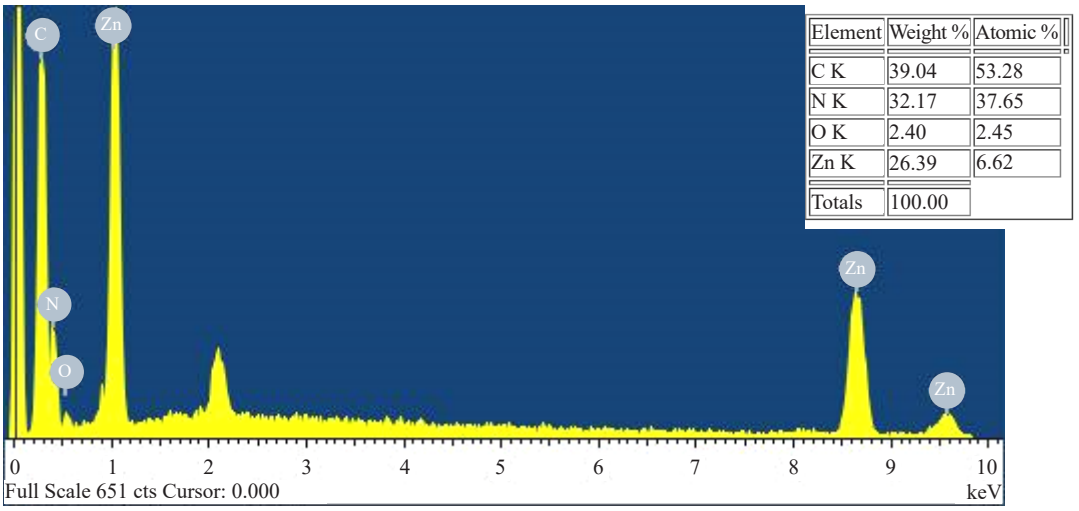


| Element | Weight % | Atomic % |
|---|---|---|
| C K | 39.04 | 53.28 |
| N K | 32.17 | 37.65 |
| O K | 2.40 | 2.45 |
| Zn K | 26.39 | 6.62 |
| Totals | 100.00 | |

(b)

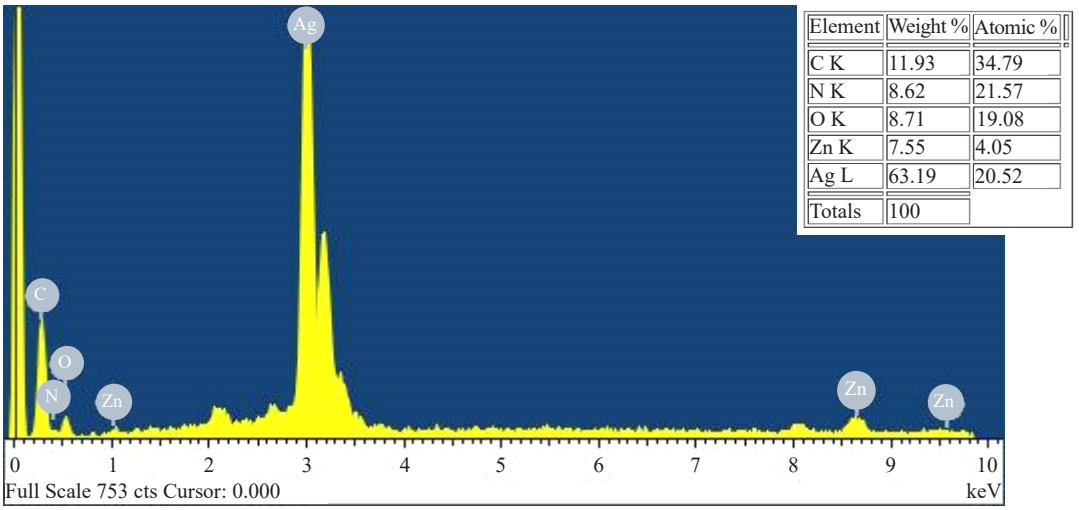


| Element | Weight % | Atomic % |
|---|---|---|
| C K | 11.93 | 34.79 |
| N K | 8.62 | 21.57 |
| O K | 8.71 | 19.08 |
| Zn K | 7.55 | 4.05 |
| Ag L | 63.19 | 20.52 |
| Totals | 100 | |

(c)

**Figure 2.** Elemental analysis (EDX) spectrum of (a) BC@Ag, (b) ZIF-8, (c) BC@Ag-MOF

# 3. Results and discussion

## 3.1 *Synthesis and characterization of BC@Ag-MOF*

In this study, BC as wound healing has been modified by the addition of immobilized silver into ZIF-8 matrix. The synthesis of this composite was carried out by mixing $AgNO_3$ and ZIF-8 solutions (ratio 1:1) with various concentrations by rapid stirring at room temperature. Furthermore, the modified material was characterized using SEM/EDX and FTIR to confirm the structure and morphology of the material.

Figure 1 shows the morphology and structure of various modified BC by SEM analysis. Bacterial cellulose has a smooth fibril-like structure with a nanometer size as shown in Figure 1a. The addition of silver ions caused the morphology of the cellulose to become rough due to the attachment of silver particles on the surface. Figure 1b indicates the SEM analysis of BC@Ag before being incubated into *E. coli* solution where silver nanoparticles (AgNPs) had not been formed. The formation of ZIF-8 crystals varied with the duration of synthesis process.[37] SEM has confirmed the morphology of ZIF-8 with rhombic dodecahedron shape and a crystal size about 400-600 nm obtained after 24 h of reaction time (Figure 1c). For SEM analysis of BC@Ag-MOF, the BC surface was covered by Ag and MOF particles uniformly (Figure 1d). The result was evidenced by the presence of Zinc (Zn) and Ag elements in the EDX analysis (Figure 2c). Interestingly, the modified cellulose (BC@Ag-MOF) exhibited a greater silver content (63.19%) than BC@Ag without immobilization into MOF (48.46%). Therefore, it can be proven that MOF has large pores for increasing the silver ion absorption capacity in BC, as conducted by previous studies.[38,39]

The functional groups of modified bacterial cellulose were confirmed using FTIR analysis as shown in Figure 3. The composite of BC@Ag-MOF consists of ZIF-8 compounds, for example, absorption bands at 3,092.08 $cm^{-1}$ and 2,927.20 $cm^{-1}$ which indicate C-H stretching. The band at 1,577.20 $cm^{-1}$ is associated with C = N stretching of imidazole ring, while the band at 422.32 $cm^{-1}$ exhibits N-Zn stretching. The band at 1,307.20 $cm^{-1}$ shows the C-H bending vibration of $-CH_3$ and the band at 984.64 $cm^{-1}$ is associated with the N-H swing. The position of this band is similar to previous research.[40,41] Furthermore, the bands at 1,464.88 $cm^{-1}$ and 1,165.36 $cm^{-1}$ indicate the bending of the O-H group and the C-O group (-glycosidic bond) which is characteristic of cellulose. The addition of Ag ions also gives a band at 1,382.80 $cm^{-1}$ which exhibits a C-N group.

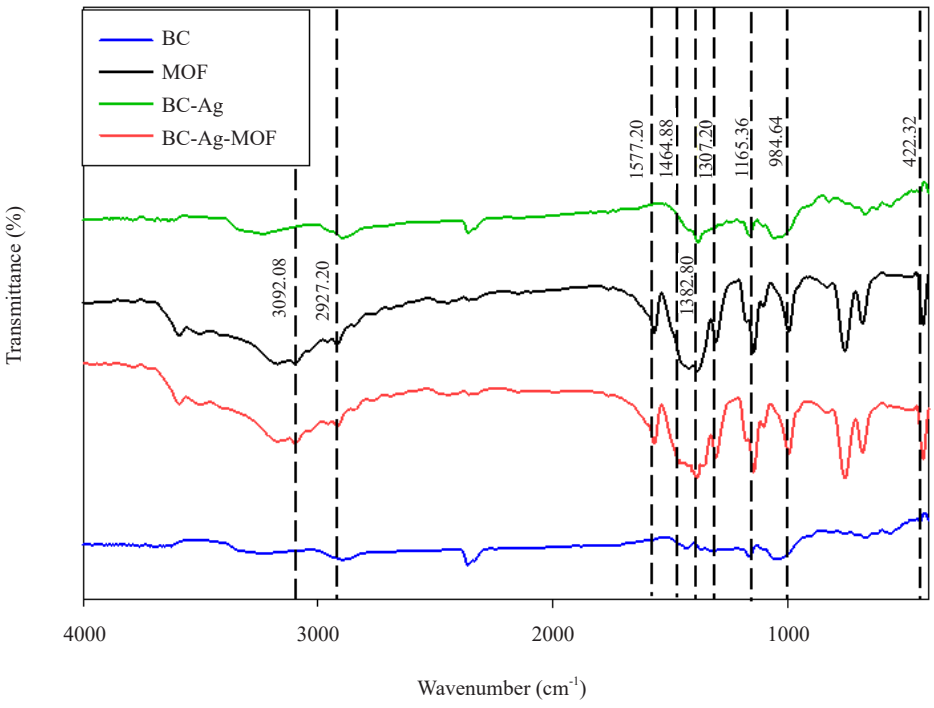


**Figure 3.** FTIR spectrum of modified bacterial cellulose

### 3.2 *Antibacterial activity against Escherichia coli*

The antibacterial activity of materials against Gram-negative *E. coli* was performed by disc diffusion and CFU methods. For disc diffusion method (Figure 4), BC@Ag-MOF has the largest inhibition zone (28.98 mm ± 0.11) compared to BC@Ag (27.13 mm ± 0.07). Whereas the inhibition zone of BC sample as control was much smaller. Additionally, it was found that $Ag^{+}$ ions in BC@Ag-MOF accepted electrons and were reduced ($Ag^{0}$) to AgNPs through enzymes secreted by *E. coli*.[42,43] Figure 4 shows the appearance of brownish color in the BC pellicle where the BC@Ag-MOF sample exhibited darker color than BC@Ag without MOF. Therefore, AgNPs were successfully immobilized into the MOF matrix, which was characterized by increased uptake of these nanoparticles into the BC, thereby enhancing the antibacterial efficacy.

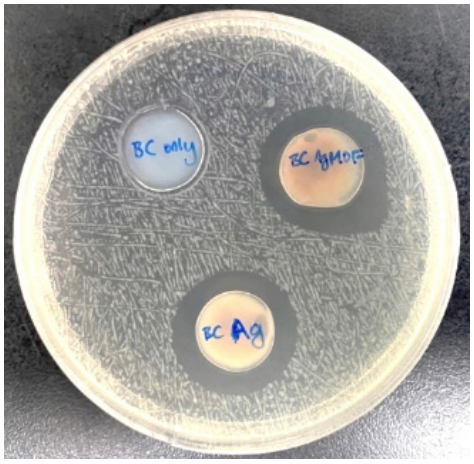


**Figure 4.** Antibacterial activity of modified bacterial cellulose by disc diffusion method. BC@Ag and BC@Ag-MOF were performed using concentration of 25 mM and incubation time of all samples was 2 hours in *E. coli* solution

The antibacterial activity by the CFU method was carried out using various concentrations of $AgNO_3$ and MOF (5, 15, 25 mM), as well as incubation time of the samples into *E. coli* solution (30, 60, 120 min). *E. coli* and BC were used as experimental controls because both samples did not have antibacterial activity. According to the results, the higher concentration of both materials and the longer incubation time of samples caused the higher reduction of bacteria (CFU/mL) due to an increase in silver absorption into the BC pellicle (Figure 5). It is known that silver nanoparticles can release silver ions continuously. Silver ions can enter the bacterial cell membrane and bind to membrane proteins that are responsible for the transport of substances in and out of the bacterial cell. In addition, silver ions are also transported into the cell and will block cell division by binding to DNA. Furthermore, the respiration of the bacteria would be disturbed and thus destroy the energy production of the cell. Eventually, the bacterial cell membrane will break and result in bacterial death.[44] Here, BC@Ag-MOF sample had the highest percentage of bacterial reduction up to 99.99% at the concentration of 25 mM and incubation time of 2 hours. This result proved that the immobilization of AgNPs into the BC matrix could increase the stability of silver ions release, thus enhancing the antibacterial activity. Under optimum conditions, 25 mM of BC@Ag and BC@Ag-MOF showed antibacterial activity results of 79 CFU/mL and 2.4 CFU/mL, indicating the efficiency of BC@Ag-MOF was 97% higher than BC@Ag.

## 4. Conclusions

In this work, the composite material (BC@Ag-MOF) exhibited a high antibacterial efficiency against Gram-negative *Escherichia coli* up to 99.99% at concentrations of 25 mM of Ag-MOF after 2 h incubation. Interestingly, the presence of MOFs matrix could release silver ions continuously in modified BC thereby enhancing the antibacterial

activity compared to BC without MOF (BC@Ag). This study showed that BC@Ag-MOF has the potential as a promising antibacterial wound healing, especially in the biomedical applications. For further study, bacterial cellulose can be modified with various types of MOFs (HKUST-1, UiO-66, MIL-100, etc.) for metal nanoparticles immobilization to increase the stability of metal ions resulting in higher antibacterial activity.

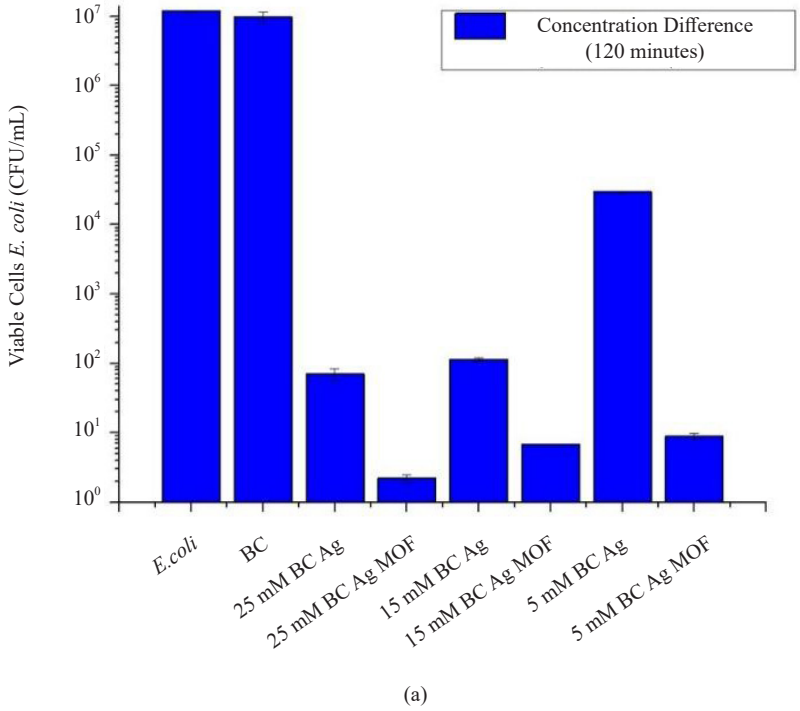


(a)

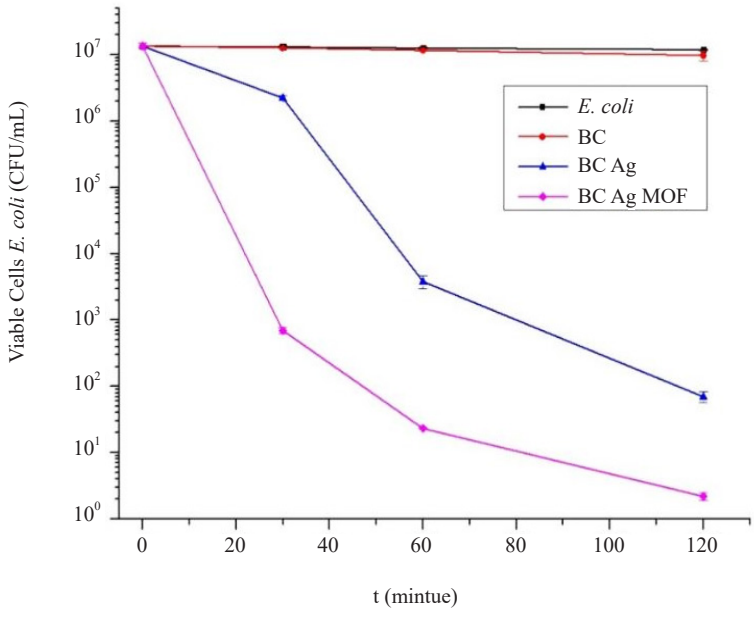


(b)

**Figure 5.** Antibacterial activity (CFU/mL) using variations of (a) materials concentration and (b) incubation time in *E. coli* solution

## Acknowledgements

Authors thank for the financial support from the Ministry of Education, Culture, Research, and Technology of the Republic of Indonesia (Grant numbers 268N/WM01.5/N/2023). The authors also thank the Research Institute and Community Service of Widya Mandala Surabaya Catholic University and Biomolecular Engineering Laboratory at National Taiwan University of Science and Technology.

## Conflict of interest statement

The authors declare no conflict of interest.

## References

[1] Almeida, A. P. C.; Saraiva, J. N.; Cavaco, G.; Portela, R. P.; Leal, C. R.; Sobral, R. G.; Almeida, P. L. Crosslinked bacterial cellulose hydrogels for biomedical applications. *Eur. Polym. J*. **2022,** *177*, 111438.

[2] Xie, Y.; Qiao, K.; Yue, L.; Tang, T.; Zheng, Y.; Zhu, S.; Yang, H.; Fang, Z. A self-crosslinking, double-functional group modified bacterial cellulose gel used for antibacterial and healing of infected wound. *Bioact. Mater*. **2022,** *17*, 248-260.

[3] Hur, D. H.; Choi, W. S.; Kim, T. Y.; Lee, S. Y.; Park, J. H.; Jeong, K. J. Enhanced production of bacterial cellulose in *Komagataeibacter Xylinus* via tuning of biosynthesis genes with synthetic RBS. *J. Microbiol. Biotechnol*. **2020,** *30*, 1430-1435.

[4] Zhou, C.; Yang, Z.; Xun, X.; Ma, L.; Chen, Z.; Hu, X.; Wu, X.; Wan, Y.; Ao, H. De novo strategy with engineering a multifunctional bacterial cellulose-based dressing for rapid healing of infected wounds. *Bioact. Mater*. **2022,** *13*, 212-222.

[5] Puspitasari, N.; Lee, C. K. Class I hydrophobin fusion with cellulose binding domain for its soluble expression and facile purification. *Int. J. Biol. Macromol*. **2021,** *193*, 38-43.

[6] Samyn, P.; Meftahi, A.; Geravand, S. A.; Heravi, M. E. M.; Najarzadeh, H.; Sabery, M. S. K.; Barhoum, A. Opportunities for bacterial nanocellulose in biomedical applications: Review on biosynthesis, modification and challenges. *Int. J. Biol. Macromol*. **2023,** *231*, 123316.

[7] Almeida do Nascimento, H.; Didier Pedrosa Amorim, J.; José Galdino da Silva Júnior, C.; D'Lamare Maia de Medeiros, A.; Fernanda de Santana Costa, A.; Carla Napoleão, D.; Maria Vinhas, G.; Asfora Sarubbo, L. Influence of gamma irradiation on the properties of bacterial cellulose produced with concord grape and red cabbage extracts. *Curr. Res. Biotechnol*. **2022,** *4*, 119-128.

[8] Zagaglia, C.; Ammendolia, M. G.; Maurizi, L.; Nicoletti, M.; Longhi, C. Urinary tract infections caused by uropathogenic *Escherichia Coli* strains - new strategies for an old pathogen. *Microorganisms*. **2022,** *10*, 1425.

[9] Lan, J.; Chen, J.; Zhu, R.; Lin, C.; Ma, X.; Cao, S. Antibacterial and antiviral chitosan oligosaccharide modified cellulosic fibers with durability against washing and long-acting activity. *Int. J. Biol. Macromol*. **2023,** *231*, 123587.

[10] Song, S.; Liu, Z.; Abubaker, M. A.; Ding, L.; Zhang, J.; Yang, S.; Fan, Z. Antibacterial polyvinyl alcohol/bacterial cellulose/nano-silver hydrogels that effectively promote wound healing. *Mater. Sci. Eng. C*. **2021,** *126*, 112171.

[11] Anwar, Y.; Ul-Islam, M.; Mohammed Ali, H. S. H.; Ullah, I.; Khalil, A.; Kamal, T. Silver impregnated bacterial cellulose-chitosan composite hydrogels for antibacterial and catalytic applications. *J. Mater. Res. Technol.* **2022,** *18*, 2037-2047.

[12] Bordiwala, R. V. Green synthesis and applications of metal nanoparticles - A review article. *Results. Chem*. **2023,** *5*, 100832.

[13] Naseem, T.; Durrani, T. The role of some important metal oxide nanoparticles for wastewater and antibacterial applications: A review. *JECE.* **2021,** *3*, 59-75.

[14] Chouke, P. B.; Shrirame, T.; Potbhare, A. K.; Mondal, A.; Chaudhary, A. R.; Mondal, S.; Thakare, S. R.; Nepovimova, E.; Valis, M.; Kuca, K.; Sharma, R.; Chaudhary, R. G. Bioinspired metal/metal oxide nanoparticles: A road map to potential applications. *Mater. Today. Adv*. **2022,** *16*, 100314.

[15] Noah, N. M.; Ndangili, P. M. Green synthesis of nanomaterials from sustainable materials for biosensors and drug

delivery. *Sens*. **2022,** *3*, 100166.
[16] Abdullah; Al-Radadi, N. S.; Hussain, T.; Faisal, S.; Ali Raza Shah, S. Novel biosynthesis, characterization and bio-catalytic potential of green algae (Spirogyra Hyalina) mediated silver nanomaterials. *Saudi. J. Biol. Sci*. **2022,** *29*, 411-419.
[17] Osorio Echavarría, J.; Gómez Vanegas, N. A.; Orozco, C. P. O. Chitosan/carboxymethyl cellulose wound dressings supplemented with biologically synthesized silver nanoparticles from the ligninolytic fungus anamorphous *Bjerkandera sp*. R1. *Heliyon*. **2022,** *8*, E10258.
[18] Singh, R.; Sagar, N. A.; Kumar, N. Bio-inspired green fabrication of silver banoparticles (AgNPs) using aqueous leaves extract of ipomoea carnea jacq. To tackle multiple drug resistance MTCC bacterial strains. *Eur. J. Med. Chem*. **2022,** *6*, 100066.
[19] Ziai, Y.; Rinoldi, C.; Nakielski, P.; de Sio, L.; Pierini, F. Smart plasmonic hydrogels based on gold and silver nanoparticles for biosensing application. *Curr. Opin. Biomed. Eng*. **2022,** *24*, 100413.
[20] Ali, Z. H.; Al-Fatlawi, A. H. Efficiency of silver nano particles in removing *Escherichia Coli* ATCC 25922 from drinking water distribution pipes. *RINENG*. **2023,** *17*, 100988.
[21] Gasaymeh, S. S.; ALmansoori, N. N. Novel formation mechanism of Ag/PANI/PVP core-shell nanocomposites. *Results. Phys*. **2020,** *16*, 102882.
[22] Chen, F.; Shen, K.; Chen, J.; Yang, X.; Cui, J.; Li, Y. General immobilization of ultrafine alloyed nanoparticles within metal-organic frameworks with high loadings for advanced synergetic catalysis. *ACS Cent. Sci*. **2019,** *5*, 176-185.
[23] Xiang, W.; Zhang, Y.; Lin, H.; Liu, C. J. Nanoparticle/metal-organic framework composites for catalytic applications: Current status and perspective. *Molecules*. **2017,** *22*, 2103.
[24] Han, Y.; Xu, H.; Su, Y.; Xu, Z. L.; Wang, K.; Wang, W. Noble metal (Pt, Au@Pd) nanoparticles supported on metal organic framework (MOF-74) nanoshuttles as high-selectivity $CO_2$ conversion catalysts. *J. Catal*. **2019,** *370*, 70-78.
[25] Mohan, B.; Singh, G.; Pombeiro, A. J. L.; Solovev, A. A.; Sharma, P. K.; Chen, Q. Metal-organic frameworks (MOFs) for milk safety and contaminants monitoring. *Trends Analyt. Chem*. **2023,** *159*, 116921.
[26] Mohan, B.; Ma, S.; Kumar, S.; Yang, Y.; Ren, P. Tactile sensors: Hydroxyl decorated silver metal-organic frameworks for detecting $Cr_2O_7^{2-}$, $MnO_4^-$, humic acid, and $Fe^{3+}$ ions. *ACS Appl. Mater. Interfaces*. **2023,** *15*, 17317-17323.
[27] Mohan, B.; Priyanka; Singh, G.; Chauhan, A.; Pombeiro, A. J. L.; Ren, P. Metal-Organic Frameworks (MOFs) based luminescent and electrochemical sensors for food contaminant detection. *J. Hazard. Mater*. **2023,** *453*, 131324.
[28] Mohan, B.; Kumari, R.; Virender; Singh, G.; Singh, K.; Pombeiro, A. J. L.; Yang, X.; Ren, P. Covalent Organic Frameworks (COFs) and Metal-Organic Frameworks (MOFs) as electrochemical sensors for the efficient detection of pharmaceutical residues. *Environ. Int*. **2023,** *175*, 107928.
[29] Wang, H.; Yu, S.; Gao, T.; Tan, X.; Meng, X.; Xiao, S. The efficient degradation of organic pollutants by Z-scheme MIL-88A@$TiO_2$ heterojunction photo-fenton catalyst: The synergistic effect of photocatalysis and fenton catalysis. *J. Alloys. Compd*. **2023,** *960*, 170688.
[30] Gao, T.; Yu, S.; Wang, H.; Zhao, X.; Wang, C.; Xiao, S. MOFs-based photocatalytic self-cleaning membranes for highly efficient wastewater treatment: A review. *Chem. Eng. Sci*. **2023,** *278*, 118891.
[31] Xiao, S.; Huo, X.; Fan, S.; Zhao, K.; Yu, S.; Tan, X. Design and synthesis of Al-MOF/PPSU mixed matrix membrane with pollution resistance. *Chin. J. Chem. Eng*. **2021,** *29*, 110-120.
[32] Naghdi, S.; Shahrestani, M. M.; Zendehbad, M.; Djahaniani, H.; Kazemian, H.; Eder, D. Recent advances in application of Metal-Organic Frameworks (MOFs) as adsorbent and catalyst in removal of Persistent Organic Pollutants (POPs). *J. Hazard. Mater*. **2023,** *442*, 130127.
[33] Mahajan, S.; Lahtinen, M. Recent progress in Metal-Organic Frameworks (MOFs) for $CO_2$ capture at different pressures. *J. Environ. Chem. Eng*. **2022,** *10*, 108930.
[34] Bergaoui, M.; Khalfaoui, M.; Awadallah-F, A.; Al-Muhtaseb, S. A review of the features and applications of ZIF-8 and its derivatives for separating $CO_2$ and isomers of $C_{3-}$ and $C_{4-}$ hydrocarbons. *J. Nat. Gas Sci. Eng*. **2021,** *96*, 104289.
[35] Jiang, S.; Li, W.; Liu, J.; Jiang, J.; Zhang, Z.; Shang, W.; Peng, N.; Wen, Y. ZnO@ZIF-8 Core-shell structure nanorods superhydrophobic coating on magnesium alloy with corrosion resistance and self-cleaning. *J. Magnes. Alloy*. **2022**.
[36] Etxeberria-Benavides, M.; Johnson, T.; Cao, S.; Zornoza, B.; Coronas, J.; Sanchez-Lainez, J.; Sabetghadam, A.;

Liu, X.; Andres-Garcia, E.; Kapteijn, F.; Gascon, J.; David, O. PBI mixed matrix hollow fiber membrane: Influence of ZIF-8 filler over $H_2/CO_2$ separation performance at high temperature and pressure. *Sep. Purif. Technol*. **2020,** *237*, 116347.

[37] Bergaoui, M.; Khalfaoui, M.; Awadallah-F, A.; Al-Muhtaseb, S. A review of the features and applications of ZIF-8 and its derivatives for separating $CO_2$ and isomers of $C_{3-}$ and $C_{4-}$ hydrocarbons. *J. Nat. Gas. Sci. Eng*. **2021,** *96*, 104289.

[38] Zhang, M.; Wang, D.; Ji, N.; Lee, S.; Wang, G.; Zheng, Y.; Zhang, X.; Yang, L.; Qin, Z.; Yang, Y. Bioinspired design of sericin/chitosan/Ag@mof/go hydrogels for efficiently combating resistant bacteria, rapid hemostasis, and wound healing. *Polymers (Basel)*. **2021,** *13*, 2812.

[39] Duan, C.; Meng, J.; Wang, X.; Meng, X.; Sun, X.; Xu, Y.; Zhao, W.; Ni, Y. Synthesis of novel cellulose-based antibacterial composites of Ag nanoparticles@ Metal-Organic Frameworks@ carboxymethylated fibers. *Carbohydr. Polym*. **2018,** *193*, 82-88.

[40] Lee, S.; Lei, Y.; Wang, D.; Li, C.; Cheng, J.; Wang, J.; Meng, W.; Liu, M. The study of Zeolitic Imidazolate Framework (ZIF-8) doped polyvinyl alcohol/starch/methyl cellulose blend film. *Polymers (Basel)*. **2019,** *11*, 1986.

[41] Rahmati, Z.; Abdi, J.; Vossoughi, M.; Alemzadeh, I. Ag-doped magnetic metal organic framework as a novel nanostructured material for highly efficient antibacterial activity. *Environ. Res*. **2020,** *188*, 109555.

[42] Ovais, M.; Khalil, A. T.; Ayaz, M.; Ahmad, I.; Nethi, S. K.; Mukherjee, S. Biosynthesis of metal nanoparticles via microbial enzymes: A mechanistic approach. *Int. J. Mol. Sci.* **2018,** *19*, 4100.

[43] Saravanan, M.; Barik, S. K.; MubarakAli, D.; Prakash, P.; Pugazhendhi, A. Synthesis of silver nanoparticles from bacillus brevis (NCIM 2533) and their antibacterial activity against pathogenic bacteria. *Microb. Pathog*. **2018,** *116*, 221-226.

[44] Yin, I. X.; Zhang, J.; Zhao, I. S.; Mei, M. L.; Li, Q.; Chu, C. H. The antibacterial mechanism of silver nanoparticles and its application in dentistry. *Int. J. Nanomedicine*. **2020,** *15*, 2555-2562.